

Dead Reckoning Navigation with Constant Velocity Update (CUPT)

Yan Li

*Faculty of Engineering
and Information
Technology
University of Technology,
Sydney
NSW 2007, Australian*
Yan.Li-
11@student.uts.edu.au

Jianguo Jack Wang

*Faculty of Engineering
and Information
Technology
University of Technology,
Sydney
NSW 2007, Australian*
Jwang@eng.uts.edu.au

Size Xiao

*School of Aerospace,
Mechanical and
Mechatronic Engineering
University of Sydney
NSW 2006, Australian*
Sxia6723@uni.sydney.edu
u.au

Xiang Luo

*Faculty of Engineering
and Information
Technology
University of Technology,
Sydney
NSW 2007, Australian*
Xiang.Luo@student.uts.e
du.au

Abstract—This paper introduces a new algorithm for dead reckoning navigation named Constant Velocity Update (CUPT), which is an extension of popular Zero Velocity Update (ZUPT). With a low-cost IMU (Inertial Measurement Unit) attached to a user's shoe, the proposed algorithm can efficiently reduce IMU errors by detecting not only the stance phases during walking, but also the cases at constant velocity, such as in an elevator or on an escalator. The concept, design and test of a CUPT prototype are detailed in this paper. Test results show that it can effectively detect constant velocity, and its horizontal positioning errors are below 0.45% of the total distance travelled, and vertical errors below 0.25%. This performance reached the highest accuracy in available literature.

Keywords— dead reckoning, ZUPT, EKF, CUPT

I. INTRODUCTION

Seamless navigation in all circumstances, including GPS (Global Positioning System) signal degraded environments, is a challenge issue. With the development of robots, robust tracking and navigation is eagerly demanded. Robots are often deployed in indoor environments where the GPS signal is unreliable. Not depending on any surrounding information, dead reckoning can provide continuous navigation information but with accumulated errors, which needs to be corrected by other measurements.

Integration of GPS and IMU has got much attention in navigation applications. Developed technologies have made it possible to use GPS in indoor environments. Godha and Lchappelle proposed a system that combined shoe-mounted IMU and GPS to bound drift errors in outdoor scenarios. The system has the ability of using IMU to bridge the navigation solution in indoors and severely signal degraded forest environments [1].

There are some non-GPS approaches to track and navigate personal position which normally require external references. Hisashi et al. [2] proposed an image sequence matching technique for the recognition of locations and previously visited places. Work is also being done on simultaneous location and mapping (SLAM), which usually uses camera or LIDAR (Light Detection And Ranging) as sensors. However, unlike inertial sensor, these sensors above are very sensitive to

the environment and are not reliable in unfavourable operation conditions.

Many approaches have been developed for pedestrian dead reckoning (PDR) [2]-[18], which do not need external devices, and can also be applied to pedal robots. The main advantage of inertial sensor-based systems is that they are self-contained, environment-independent and can provide instantaneous position, velocity and attitude measurements. The major challenge for PDR is to efficiently reduce or bound navigation errors.

There are many different PDR systems using inertial sensors. The simplest one is the pedometer, which counts steps and estimates average length of steps. Cho and Park [3] proposed a pedometer-like approach which uses a two-axis accelerometer and a two-axis magnetometer attached to user's boot. Step length is estimated from the accelerometers readings that are passed through a neural network, and a Kalman Filter was used to reduce the effect of magnetic disturbances. While the results in outdoors are reasonable, the results in indoor environment have large errors as the varying magnetic disturbances.

As a special character for pedestrian, there are stance phases during walking, which can be used for PDR drift correction. Therefore, various ZUPT algorithms for PDR navigation have been developed [4-17]. Algorithms for step detection using accelerometers have been presented, which mainly contain three types: peak detection, zero crossing detection and flat zone detection [4]. In [5], a gait state is modelled as a Markov process and gait states are estimated using the hidden Markov model filter based on force sensors to determine when to apply ZUPT. Similarly, a Markov model is constructed using segmentation of gyroscope outputs in [6]. Slightly different algorithms can be achieved based on both accelerometer and gyroscope outputs. In [7], the zero velocity is determined by comparing z-axis accelerometer and y-axis gyroscope outputs with the threshold value. In [8], the zero velocity is determined based on norms of accelerometer and gyroscope along with variance of accelerometer.

All the above detectors can be generalized as the so-called acceleration moving variance detector, the acceleration

magnitude detector, the angular rate energy (ARE) detector which are all generalized likelihood ratio tests. Skog et al. [10] developed a novel stance hypothesis optimal detector; however, it is restricted to 2D cases. Ojeda and Borenstein et al. [11] proposed a shoe-based navigation system consists of a 15-state error model. Their system works well in both 2D and 3D environments. With the ARE detector and related signal processing algorithms, the horizontal relative error was about 0.49% of the total distance travelled, but the vertical error was always more than 1%.

None of the algorithms mentioned above, however, can perform well in situations with consistent velocity, such as in an elevator or on an escalator. This is due to the fact that they detect the cases with constant velocity as zero velocity. This paper proposes an improved shoe-mounted PDR system, and proposes a new algorithm named CUPT. It can detect not only the stance phases as ZUPT, but also constant velocity when a user is standing in an elevator or on an escalator. A model with 24 error states is applied to correct IMU errors with Extended Kalman Filter (EKF). Experimental results show that the positioning accuracy of the proposed system is better than 0.45% in horizontal plane, and 0.25% in vertical. It is better or comparable to some of the highest positioning accuracy figures reported for ZUPT[11], [12] and [16].

II. MATHEMATICAL MODELLING

An IMU normally consists of three accelerometers and three gyroscopes in an orthogonal pattern. The standard strapdown inertial navigation system (INS) mechanization is used in our system.

A. Strapdown Inertial Navigation Mechanization

Figure1 shows strapdown INS mechanization. Attitude can be determined by integration of the rotation rate of gyros. After vector transformation, velocity and position can be determined by the integration of acceleration with compensation of gravity and Coriolis force. Details of the blocks can be seen in [9] and [18].

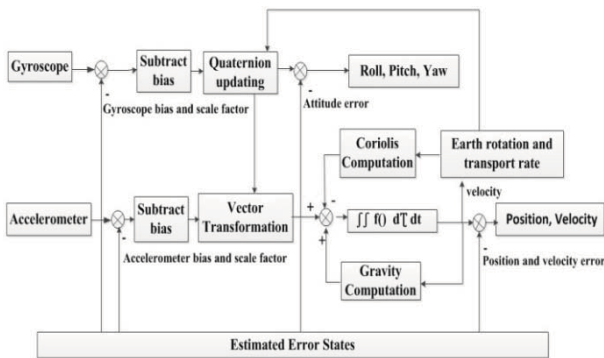


Figure1. The basic blocks of strapdown INS mechanization

In practice, however, this simple integration will lead to unbounded growth in position errors with time due to the noise associated with the measurement and the non-linearity of the sensors. In order to get high accuracy navigation solution with IMU, the technique ZUPT is applied to reduce errors.

B. ZUPT

When a person walks, his feet alternate between a stationary phase and a swing phase. This stance interval appears in each step at zero velocity, thus the velocity errors can be reset almost periodically. It is important to identify the stance intervals when the sensors attached to the shoe are stationary and then apply ZUPT to bind the errors with EKF. In each estimation cycle, once zero velocity has been detected, ZUPT delivers the updated error states to INS, otherwise, the error states use the ones which are updated in the last stance interval. ZUPT can not only correct velocity, but also help to restrict correlated position and attitude errors and estimating the sensor bias errors. Figure2 shows the main blocks in a typical INS-EKF-ZUPT PDR methodology [8].

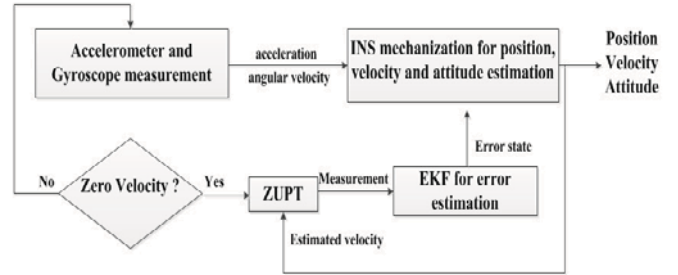


Figure2. The main blocks in the framework used for pedestrian dead-reckoning.

C. CUPT

In principle, all the instants that are correctly detected can be applied to EKF estimated error states correction, including but not limited to zero velocity. Here constant velocity is tackled; therefore the algorithm is called CUPT. The proposed algorithm can detect the stance phases as ZUPT when stepping on the ground, and also the constant velocity when standing in a moving elevator or on a moving escalator.

ZUPT is just a special case in CUPT when the true velocity condition is exactly zero. If a ZUPT algorithm is applied to test the cases with constant velocity, it will regard the constant velocity as zero velocity and perform ZUPT. As the result, the navigation solution is obviously wrong.

The core concept of CUPT algorithm is to detect the velocity of the standing platform and use it to correct INS drift. Obviously, without considering the velocity condition, the constant velocity phases satisfy all the conditions for zero velocity stance phases. CUPT needs to identify not only a stance phase, but also the velocity during the stance phase, and whether the velocity is constant or not.

D. Kalman Filter

An exact expression for the system equation of an EKF depends on the states selected and the type of error model used to describe them. The EKF we used includes the following 24 error states[19]:

$$\begin{aligned} \delta x_{Nav} &= [\delta r_N, \delta r_E, \delta r_D, \delta v_N, \delta v_E, \delta v_D, \delta \phi_H, \delta \phi_P, \delta \phi_R]^T \\ \delta x_{INS} &= [\nabla_b, \nabla_f, \varepsilon_b, \varepsilon_f] \\ \delta x_{Grav} &= [\delta g_N, \delta g_E, \delta g_D]^T \end{aligned} \quad (1)$$

Where δx_{Nav} , δx_{INS} and δx_{Grav} are the navigation error vector, the IMU sensor measurement error vector and gravity uncertainty, respectively. ∇ is the accelerometer error vector, and ε is the gyro error vector. Subscript b stands for bias and subscript f stands for scale factor.

Psi-angle model is adopted in the system [19]:

$$\begin{aligned}\dot{\delta r} &= -\omega_{en} \times \delta r + \delta v \\ \delta \dot{v} &= -(\omega_{ie} + \omega_{in}) \times \delta v - \delta \varphi \times f + \delta g + \nabla \\ \delta \dot{\varphi} &= -\omega_{in} \times \delta \varphi + \varepsilon\end{aligned}\quad (2)$$

Where, δr , δv and $\delta \varphi$ are the position, velocity, and attitude error vectors respectively, δg is the error in the computed gravity vector, f is the specific force vector, ω_{ie} is the earth rotation rate vector, ω_{en} is the transport rate vector and ω_{in} is the angular rate vector from the navigation to the inertial frame.

The dynamic matrix is obtained by a linearization of the equation (2). A detailed expression of the dynamic matrix can be found in [19]. The measurement model is

$$z = H\delta x + n \quad (3)$$

Where $H = [0 \ 1 \ 0 \ 0 \ 0 \ 0 \ 0]$, n is the measurement noise.

Consider the error state $\delta x = \hat{x} - x$, where \hat{x} is the estimated state and x is the true state, the observation z for constant velocity is $\hat{x} - V$ and $\hat{x} - 0$ for zero velocity, where \hat{x} is computed by the strapdown inertial computer.

In this approach, the crucial issue for achieving good navigation performance is to get reliable and robust stance phase detection for both zero and constant velocity.

III. STANCE PHASE DETECTION

CUPT is applied in the EKF if the detector decides that the foot is stationary. Here “stationary” means not only that the foot is contacted with ground and not moving, but also keeps static relative to the moving platform. Whatever update technique is applied, the characteristic of the sensor outputs is the same, for this reason, the stance phase for both cases can be detected using the zero-velocity detector.

In the proposed approach, it is not necessary to identify the exact start and end of a stance interval. Rather, as long as one single instance in a stride is detected, it can be used to remove the sensor drift, so the error will not be accumulated. The stance interval detector which is introduced in our paper uses both accelerometer and gyro measurements in real-time conditions. The algorithm implemented consists of the following 4 conditions:

- 1) The magnitude of the acceleration $|a_k|$, for every sample k :

$$\begin{aligned}|a_k| &= \left[a_{xk}^2 + a_{yk}^2 + a_{zk}^2 \right]^{0.5} \\ C1 &= \begin{cases} 1 & th_{a \min} < |a_k| < th_{a \max} \\ 0 & otherwise \end{cases}\end{aligned}\quad (4)$$

- 2) The magnitude of the acceleration on z axis $|a_{kz}|$, for every sample k :

$$C2 = \begin{cases} 1 & th_{az \min} < |a_{kz}| < th_{az \max} \\ 0 & otherwise \end{cases} \quad (5)$$

- 3) The magnitude of the gyroscope $|\omega_k|$, for every sample k :

$$\begin{aligned}|\omega_k| &= \left[\omega_{xk}^2 + \omega_{yk}^2 + \omega_{zk}^2 \right]^{0.5} \\ C3 &= \begin{cases} 1 & |\omega_k| < th_{\omega \max} \\ 0 & otherwise \end{cases}\end{aligned}\quad (6)$$

- 4) The magnitude of the gyroscope on y axis $|\omega_{ky}|$, for every sample k :

$$C4 = \begin{cases} 1 & |\omega_{ky}| < th_{\omega y \max} \\ 0 & otherwise \end{cases} \quad (7)$$

The z axis acceleration and the y axis angular velocity are the most significant indicators of a walking event. Since a foot in contact with ground indicates a stance interval, the acceleration of gravity and the angular rate of foot rotation do not vary over this duration. However, due to unsteady tilt of the shoe surface, the measured ω_y and a_z are not exactly 0 and g respectively. Moreover, in ideal condition, the magnitude of total angular velocity and acceleration on horizontal plane should be zero in a stance phase; but in fact, they will not be zero, but a lower value than a given threshold. The thresholds are based on the average value of the accelerometer and gyro outputs during the initial stationary period of time plus a certain level of fluctuation to ensure its robustness. The initial stationary period is at the beginning of sensor data collection when the IMU is in a stable condition.

These four logical conditions must be satisfied simultaneously to declare a foot as stationary. In addition, another threshold of time period should be used to prevent some zero-crossings in swing phase from being mistakenly detected. Here we set a fixed sample window with a size of 5. Once a sample is detected as stance phase, and the next consecutive four samples are all detected to be stance phase, CUPT is applied to reduce drift. Velocity is reset to current known condition, the position, velocity and attitude errors are reset to zero after EKF refine the current position, velocity and attitude. The accelerometer and gyro errors and gravity uncertainty are accumulated and fed back to the EKF which allows the filter to correct velocity error after each stride.

Take an elevator as example, the elevator goes through a period of acceleration and braking before it is stationary again. The constant velocity appears once the elevator finishes accelerating and before the elevator starts slowing down. In this circumstance, the most significant indicator is the acceleration on z axis.

For the case on an escalator, the horizontal velocity is the most significant indicator. As a foot steps on the escalator and afterward keeps pace with the escalator going up or down until get off, the constant (escalator) velocity is determined by the instance the foot set on the escalator. Once the horizontal velocity is over a threshold (here we set at 0.35m/s) in stance

phase, it is assumed that the foot is on an escalator and we apply CUPT as measurement of EKF. Although at different sections of an escalator, the vertical angle may be different. Here we set the angle of the escalator at 30 degrees, which could get the vertical velocity by force analysis.

Our system can also roughly estimate stride length. According to [9], when a person walks, their feet alternate between a stance phase and a moving stride phase, each lasting about 0.5 seconds. As all the samples in stance phase have been detected, we can find the position that the foot fall on the ground for each step, thus get every stride length.

IV. EXPERIMENTS

A. Hardware Description

We implement the proposed PDR algorithm with a MEMS IMU, Navchip from Intersense Incorporated. Navchip is the smallest IMU in the world and it deliveries excellent measurement results. The small size of Navchip makes it easy to attach to a boot and has no effect on walking. Table I lists the specification of Navchip (encapsulated within casing).

TABLE I SPECIFICATION OF NAVCHIP

Gyroscope Performance		Accelerometer Performance	
Range (deg/sec)	± 480	Range(m/s ²)	± 8
Noise Density (°/s/ $\sqrt{\text{Hz}}$)	0.004	Noise Density (ug/ $\sqrt{\text{Hz}}$)	70
Bias Stability (°/hr, 1 σ)	12	Bias Stability (mg, 1 σ)	0.1

We mounted the IMU on the front surface of a boot. During initial test, we discovered the phenomenon of excessive shock and acceleration measurement overflow. We took countermeasures such as placing shock absorb padding and protective casing. Tests afterwards show reduced shock and improved measurement. Figure 3 shows the accelerometer measurement before (upper figure) and after the shock countermeasure.

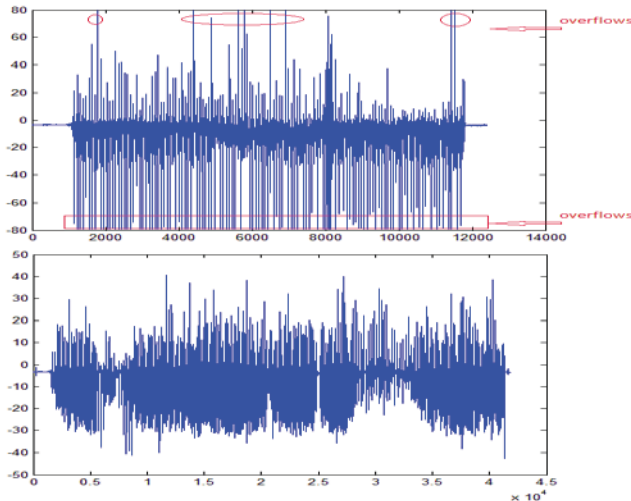


Figure3. Comparison of acceleration before and after shock reduce

The boot mounted with the IMU was worn by a pedestrian for testing. This should also hold true for pedal robots.

Therefore the subject is used to indicate the boot wearer in the following sections.

B. Tests

In this section we present results in two scenarios and all the trajectories are closed loop, which means the subject stops at the exact same location where he starts. In addition, in all cases before walking, the subject stands still at the start point for about 4 seconds.

1) Experiments in elevator

The test was conducted in a tower building which has multi elevators and 27 levels. The subject walked for a while before he went into the elevator. When the door was closed, the subject stopped walking and stayed still until the door opened again. Which level the elevator chose to stop at and which elevator chose to take are all random. Since the start (dark dot) and stop point (blue dot) are exact same location in reality, the distance between the dark and blue dot in the below figures represent the relative error.

The three trajectories are as follows:

- Start walking at level 4; take an elevator up to level 26 followed by a walking and down to level 4 by another elevator.
- Start walking at level 4; take an elevator up to level 26 followed by a walking and down to level 2 by the same elevator and then back up to level 4 by another elevator.
- Start walking at level 4, take an elevator up to level 24 and climb the stairs to level 26, go down to level 16 by another elevator, walk outside the elevator and back down to level 4.

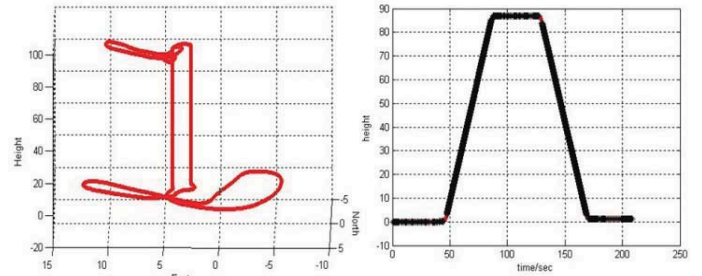


Figure4. Trajectory1 of elevator test

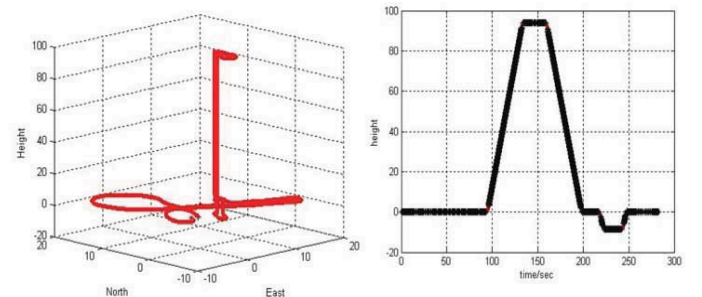


Figure5. Trajectory2 of elevator test

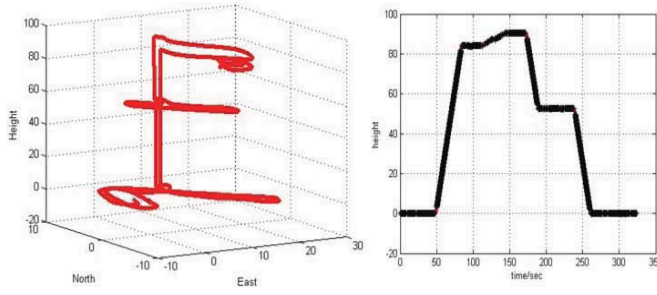


Figure6. Trajectory3 of elevator test

The left figure is the 3D view of the trajectory while the right figure represents the height changed over time drew by the red line, the black dots indicate the sample points have been applied CUP or ZUP.

2) Experiments on escalator

Starting at the lower level, the subject walked for a while and stood on an arising escalator with the IMU mounted on one foot. Then the subject got off the escalator on middle level and walked to another arising escalator to the top level, and backed down to the start point via two falling escalators.

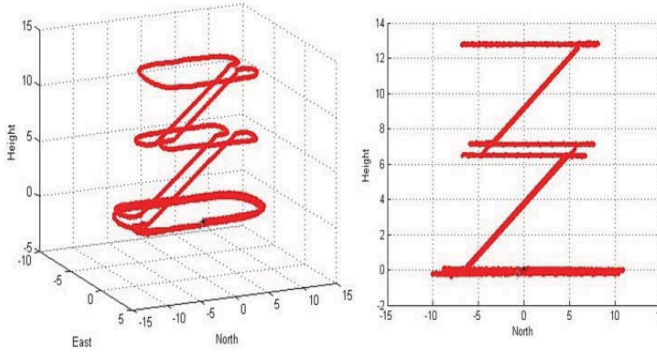


Figure7. Trajectory of escalator test

Figure 7 is the 3D view of the trajectory, which clearly represents the four escalators and the three levels walked.

V. RESULTS AND DISCUSSION

Figure 8 shows one section of CUP computed velocity for the case in an elevator. The elevator went through a period of accelerating, kept at a constant velocity, then decelerated to zero velocity. The green line draws the velocity of the vertical direction and the blue line represents the raw accelerometer measurements on z axis.

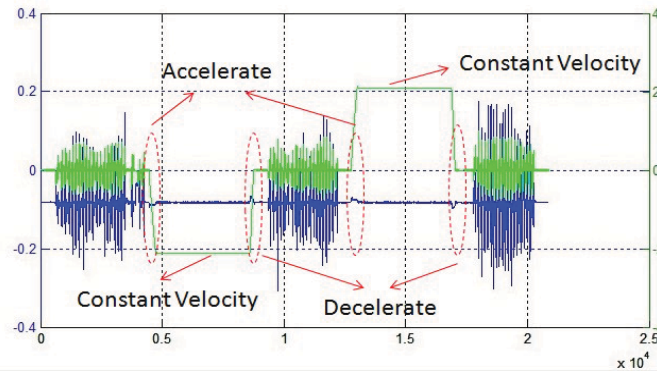


Figure8. Indication of motion in an elevator

Figure 9a shows the steps walking on the ground applied ZUP but no update for standing on the escalator, which results in large errors in velocity without IMU drift correction. Figure 9b shows one section of CUP computed velocity for the same case, which keeps at a constant velocity going along with the escalator until steps down to the ground. The black dots stand for the sample points have been detected to be constant velocity or zero velocity, the red, blue and green line draw the velocity of the north, east and vertical direction respectively.

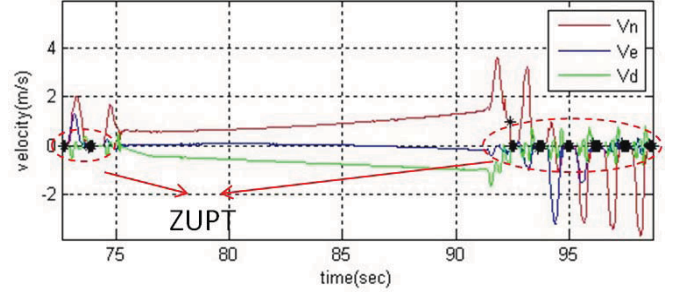


Figure9a. Motion in an escalator without update

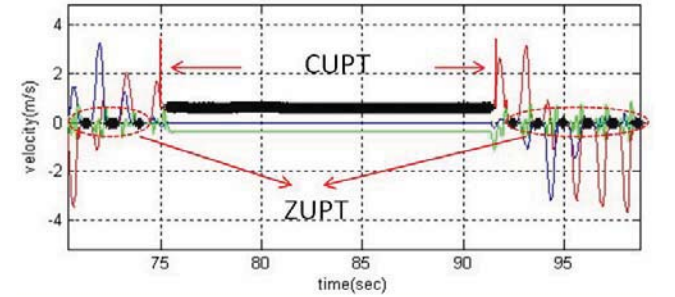


Figure9b. Motion in an escalator with CUP

Table II and III summarize the return position errors for elevator and escalator experiments respectively.

TABLE II RETURN POSITION ERRORS OF ELEVATOR

Elevator	Estimate Distance (m)	Relative (%)	
		X-Y plane	Z direction
Trajectory 1	248.3	0.17%	0.47%
Trajectory 2	324.7	0.39%	0.063%
Trajectory 3	373.0	0.56%	0.02%
Average	315.3	0.37%	0.18%

TABLE III RETURN POSITION ERRORS OF ESCALATOR

Escalator	Estimate Distance (m)	Relative (%)	
		X-Y plane	Z direction
Trajectory 1	223.3	0.34%	0.11%
Trajectory 2	259.1	0.56%	0.34%
Trajectory 3	232.4	0.64%	0.37%
Trajectory 4	210.8	0.22%	0.10%
Average	231.4	0.44%	0.23%

Although these test results are reasonably good, there is still large room to further improve the proposed algorithm to achieve better performance and handle more challenge situations. Processing elevator data during accelerating and braking sections, CUPT follows the INS mechanization computing position, velocity and attitude without any update and correction until constant velocity is detected. However, in some cases it is hard to detect constant velocity. The motion in accelerating and braking sections is with variable acceleration. Especially during braking, an elevator firstly slows down to a low speed and keeps constant for a while, then decelerates to zero velocity, which needs more specific analysis. Moreover, the frequency elevator stops also has an influence of the accuracy of height measurement. As CUPT only implements at the instance when the accelerating period ends, if an elevator stops frequently, its acceleration takes more time and is not obvious for detection, which could result in false or missing constant velocity detection.

While for escalator, the vertical angle of the escalators was predetermined to compute the vertical velocity. This angle could be measured by the sensor with more sophisticated investigation. Although the height relative error in Table III is small, the horizontal relative error is not so good. This may due to the change of vertical angle at the two ends of escalators that the staircase keeps moving forward but no longer goes upward or downward, where the predetermined angle introduces error for measurement update.

VI. CONCLUSION AND FUTURE WORK

This paper presents a CUPT algorithm for self-contained PDR system which works on moving platform with good performance. For elevator experiments, the average return position error on the horizontal plane is around 0.37% of the total distance travelled, the height drift is about 0.18%. The return position error for escalator is a little larger, that is 0.44% on horizontal plane by average and 0.23% on vertical. From the test results, we can draw a conclusion that the CUPT algorithm is very efficient to limit the growth of IMU error. Our robust stance phase detection and constant velocity update algorithm shows satisfactory performance. This CUPT algorithm could give accurate navigation solution simultaneously as a pedal robots or pedestrian is walking.

The proposed algorithm is robust in walking conditions; however, it performs not so well for some other legged locomotion, such as running or jumping, which is mainly due to the excessive shock and sensor measurement overflow. We are still working on a solution to these issues. In the future, we will investigate methods for eliminating heading error by integrating the magnetic field measurement; a more robust CUPT algorithm and specific model analysis suitable for more complicate environments.

ACKNOWLEDGMENT

The authors sincerely appreciate Professor Guang Hong for providing the sensor as well as the UTS workshop personals for manufacturing the protective casing of our sensor.

REFERENCES

- [1] S. Godha and G. Lachapelle, "Foot mounted inertial system for pedestrian navigation," *Meas. Sci. Technol.*, vol. 19 2008.
- [2] B. Schiele, *et al.*, "Realtime Personal Positioning System for Wearable Computer," presented at the 3rd IEEE International Symposium on Wearable Computers (ISWC 1999), Washington, DC, USA 1999.
- [3] S. Y. Cho and C. G. Park, "MEMS Based Pedestrian Navigation System," *Journal of Navigation*, vol. 59, pp. 135-153, 2006.
- [4] S. Y. Cho, *et al.*, "A Personal Navigation System Using Low-Cost MEMS/GPS/Fluxgate," presented at the Proceedings of the 59th Annual Meeting of The Institute of Navigation and CIGTF 22nd Guidance Test Symposium, Albuquerque, NM, 2003.
- [5] Y. S. Suh and S. Park, "Pedestrian inertial navigation with gait phase detection assisted zero velocity updating," presented at the Autonomous Robots and Agents, 2009. ICARA 2009. 4th International Conference on Autonomous Robots and Agents, Wellington, New Zealand, 2009.
- [6] S. K. Park and Y. S. Suh, "A Zero Velocity Detection Algorithm Using Inertial Sensors for Pedestrian Navigation Systems," *Sensors* vol. 10, pp. 9163-9178, 2010.
- [7] X. Yun, *et al.*, "Self-contained Position Tracking of Human Movement Using Small Inertial/Magnetic Sensor Modules," presented at the 2007 IEEE International Conference on Robotics and Automation, Roma, Italy, 2007.
- [8] A. R. Jiménez, *et al.*, "Indoor pedestrian navigation using an INS/EKF framework for yaw drift reduction and a foot-mounted IMU," presented at the 7th Workshop on Positioning Navigation and Communication (WPNC), Dresden 2010.
- [9] E. Foxlin, "Pedestrian Tracking with Shoe-Mounted Inertial Sensors," *IEEE Computer Graphics and Applications In Computer Graphics and Applications*, vol. 25, pp. 38-46, November 2005.
- [10] I. Skog, *et al.*, "Evaluation of zero-velocity detectors for foot-mounted inertial navigation systems," presented at the 2010 International Conference on Indoor Positioning and Indoor Navigation (IPIN), Zurich 2010.
- [11] L. Ojeda and J. Borenstein, "Non-GPS Navigation for Security Personnel and First Responders," *Journal of Navigation*, vol. 60, pp. 391-407, 09 August 2007.
- [12] N. Castañeda and S. Lamy-Perbal, "An improved shoe-mounted inertial navigation system," in *2010 International Conference on Indoor Positioning and Indoor Navigation (IPIN)*, Campus Science City, ETH Zurich, 2010.
- [13] C. Huang, *et al.*, "Synergism of INS and PDR in Self-Contained Pedestrian Tracking With a Miniature Sensor Module," *Sensors Journal, IEEE* vol. 10, pp. 1349-1359, Aug. 2010.
- [14] R. Feliz, *et al.*, "Pedestrian Tracking Using Inertial Sensors," *Journal of Physical Agents*, vol. 3, pp. 35-43, Jan 2009.
- [15] S. Rajagopal, "Personal dead reckoning system with shoe mounted inertial sensors," Master of Science, Electrical and Electronic Engineering KTH, Stockholm, Sweden, 2008.
- [16] O. Bebek, *et al.*, "Personal Navigation via High-Resolution Gait-Corrected Inertial Measurement Units," presented at the IEEE Transactions on Instrumentation and Measurement, 2010.
- [17] A. R. Jimenez, *et al.*, "A Comparison of Pedestrian Dead-Reckoning Algorithms Using a Low-Cost MEMS IMU," *IEEE International Symposium on Intelligent Signal Processing*, pp. 37 - 42 26-28, Aug 2009.
- [18] H. K. Lee, "Integration of GPS/Pseudolite/INS for High Precision Kinematic Positioning and Navigation," Doctor of Philosophy, School of Surveying and Spatial Information Systems, The University of New South Wales, Sydney NSW 2052, Australia, 2004.
- [19] D. A. *et al.*, "Bridging GPS Gaps in Urban Canyons: Can ZUPT Really Help?," *Proceedings of the 58th Annual Meeting of The Institute of Navigation and CIGTF 21st Guidance Test Symposium*, pp. 231-240, June 24 - 26, 2002.